On the Error Modeling of a Novel Mobile Hybrid Parallel Robot

Yongbo Wang(1,2), Huapeng Wu(1), Heikki Handroos(1), Bingkui Chen(2)

(1) Department of Mechanical Engineering
IMVE, Lappeenranta University of Technology
P.O. Box 20, FIN-53851 Lappeenranta, Finland
yongbo.wang@lut.fi, huapeng.wu@lut.fi,
hekki.handroos@lut.fi

(2) Department of Mechanical Engineering
SLMT, Chongqing University
Shapingba, Chongqing, 400044, PR. China
bkchen @cqu.edu.cn

***Abstract*—This paper presents a method for the kinematic analysis and error modeling of a newly developed hybrid redundant robot IWR (Intersector Welding Robot), which possesses ten degrees of freedom (DOF) where 6-DOF in parallel and additional 4-DOF in serial. In this article, the problem of kinematic modeling and error modeling of the proposed IWR robot are discussed. Based on the vector arithmetic method, the kinematic model and the sensitivity model of the end-effector subject to the structure parameters is derived and analyzed. The relations between the pose (position and orientation) accuracy and manufacturing tolerances, actuation errors, and connection errors are formulated. Simulation is performed to examine the validity and effectiveness of the evolutionary algorithm for the application.**

***Keywords*—accuracy, error modeling, parallel robot, kinematic analysis**

I. INTRODUCTION

Accuracy is an utmost important consideration factor when design a robot, whatever it is a serial robot or parallel robot. It is believed that parallel robot have some favorable advantages, such as higher speeds and accelerations, compact structure, and improved accuracy because the joint errors are not accumulated like in its counterpart. On the other hand, serial robots have some advantages like larger workspace, higher dexterity and good maneuverability but exhibit low stiffness and poor positioning accuracy because of their serial structures. To take advantage both of their merits, in this paper, a redundant hybrid robot which possesses both serial and parallel links will be introduced, the serial part of the machine is used to provide big work volume, while parallel links bring high loading capabilities and stiffness to the whole structure [1], thus a promising compromise of best sides of parallel kinematics and serial robots might be achieved. In the paper, based on the differentiation algorithm method, the error model of the proposed robot will be formulated.

In the past decades, there are a number of publications concerning the serial robots and parallel robots respectively. For the Hexapod, Wang and Masory [2] investigated how manufacturing and assembly errors affect the accuracy of a Hexapod by modeling the legs as serial kinematic chains using the D-H convention. Ropponen and Arai [3] presented an error model based on differentiation of the kinematics. For the serial robot, Veitschegger and Chi-haur Wu [4] developed a linear error model to determine the Cartesian position and orientation accuracy of a robot manipulator with respect to the statistical distributions of the kinematics parameters. However, very few publications dealing with hybrid robot have been found, J.-W Zhao and K.-C Fan [6] illustrated a serial-parallel type machine tool and evaluated its accuracy based on the linkage kinematic analysis and the differential vector method.

The paper is organized into four main sections. The first section serves as introduction. The second section reviews the kinematic analysis and error modeling of the proposed robot. Simulation results are presented in the third section, and conclusions are drawn in the fourth section.

II. KINEMATIC ANALYSIS AND ERROR MODELING

The kinematics of the proposed hybrid robot as shown in Fig.1 can be divided into two parts, the serial part and the parallel one, i.e., the carriage and Hexapod. To simplify its analysis, the two parts will be first carried out respectively, and then combined them together to obtain the final solutions.

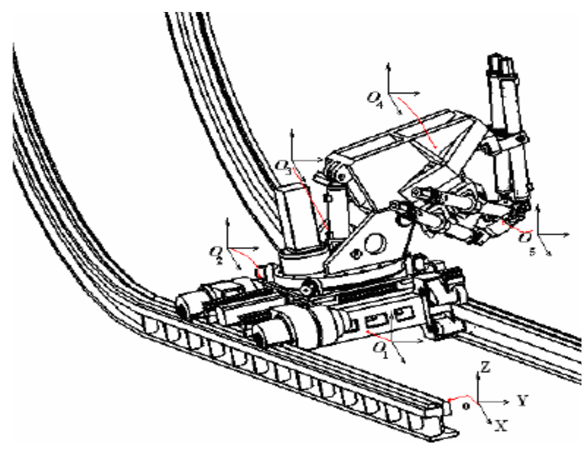

Figure 1. 3D model of IWR

A. *error modeling of the carriage*

Based on the convention of Denavit-Hartenberg coordinate system, the principle of the 4-DOF carriage mechanism is established in Fig.2, which provides four degrees of freedom at the end-effector, including two translational movements and two rotational movements.

978-1-4244-1676-9/08 /$25.00 ©2008 IEEE

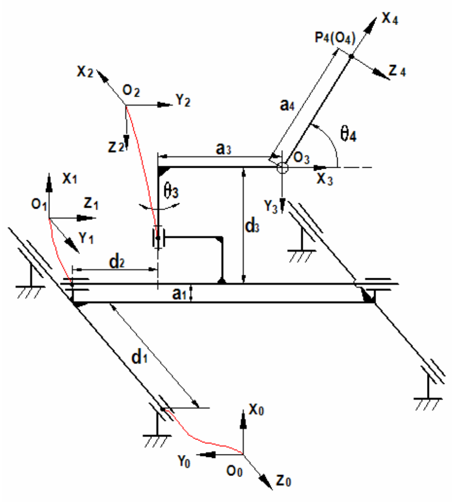

Figure 2. Coordinate system of carriage

Using the coordinate systems established in Fig. 2, the corresponding link parameters are given in Table1. Substituting the D-H link parameters into (1), we can obtain the D-H homogeneous transformation matrices ${}^{0}\mathbf{A}_1$, ${}^{1}\mathbf{A}_2$, ${}^{2}\mathbf{A}_3$ and ${}^{3}\mathbf{A}_4$.

TABLE I. D-H PARAMETERS OF CARRIAGE

Joint i	α_i	a_i	d_i	θ_i
1	$\pi/2$	a_1	d_1	0
2	$\pi/2$	0	d_2	$\pi/2$
3	$\pi/2$	a_3	d_3	θ_3
4	$-\pi/2$	a_4	0	θ_4

$$ {}^{i-1}\mathbf{A}_i = \begin{bmatrix} c\theta_i & -c\alpha_i s\theta_i & s\alpha_i s\theta_i & a_i c\theta_i \\ s\theta_i & c\alpha_i c\theta_i & -s\alpha_i c\theta_i & a_i s\theta_i \\ 0 & s\alpha_i & c\alpha_i & d_i \\ 0 & 0 & 0 & 1 \end{bmatrix} \tag{1} $$

where $c\theta_i$ denotes $\cos\theta_i$, and $s\theta_i$ denotes $\sin\theta_i$.

The resulting homogeneous transformation matrix can be obtained by multiplying the matrices of ${}^{0}\mathbf{A}_1$, ${}^{1}\mathbf{A}_2$, ${}^{2}\mathbf{A}_3$ and ${}^{3}\mathbf{A}_4$.

$$ \begin{aligned} {}^{0}\mathbf{A}_4 &= {}^{0}\mathbf{A}_1\,{}^{1}\mathbf{A}_2\,{}^{2}\mathbf{A}_3\,{}^{3}\mathbf{A}_4 \\ &= \begin{bmatrix} s\theta_4 & 0 & c\theta_4 & a_1 + d_3 + a_4 s\theta_4 \\ -s\theta_3 c\theta_4 & -c\theta_3 & s\theta_3 s\theta_4 & -d_2 - a_3 s\theta_3 - a_4 s\theta_3 c\theta_4 \\ c\theta_3 c\theta_4 & -s\theta_3 & -c\theta_3 s\theta_4 & d_1 + a_3 c\theta_3 + a_4 c\theta_3 c\theta_4 \\ 0 & 0 & 0 & 1 \end{bmatrix} \end{aligned} \tag{2} $$

Based on (2), the forward kinematics can be written as follows

$$ p_x = a_1 + d_3 + a_4 s\theta_4 \tag{3} $$

$$ p_y = -d_2 - a_3 s\theta_3 - a_4 s\theta_3 c\theta_4 \tag{4} $$

$$ p_z = d_1 + a_3 c\theta_3 + a_4 c\theta_3 c\theta_4 \tag{5} $$

The inverse kinematic model can be obtained as

$$ \theta_4 = \sin^{-1}\left(\frac{p_x - a_1 - d_3}{a_4}\right) \tag{6} $$

$$ d_1 = p_z - a_3 c\theta_3 - a_4 c\theta_3 c\theta_4 \tag{7} $$

$$ d_2 = -p_y - a_3 s\theta_3 - a_4 s\theta_3 c\theta_4 \tag{8} $$

For the accuracy of the carriage, it depends on the accuracy of the four-link parameters of each joint [4]. If there are errors in the dimensional relationships between two consecutive joint $i-1$ and i, there will be a differential change $d\,{}^{i-1}\mathbf{A}_i$ between the two joint coordinates. Therefore, the correct relationship between the two successive joint coordinates will be written as

$$ {}^{i-1}\mathbf{A}_i^c = {}^{i-1}\mathbf{A}_i + d\,{}^{i-1}\mathbf{A}_i \tag{9} $$

where ${}^{i-1}\mathbf{A}_i$ is the homogeneous matrix which have the nominal link parameters that can express the relationship between the joint coordinates $i-1$ and i, and $d\,{}^{i-1}\mathbf{A}_i$ is the differential change due to errors in the link parameters. It can be approximated as a linear function of four kinematics errors by Taylor's series:

$$ d\,{}^{i-1}\mathbf{A}_i = \frac{\partial\,{}^{i-1}\mathbf{A}_i}{\partial\theta_i}\Delta\theta_i + \frac{\partial\,{}^{i-1}\mathbf{A}_i}{\partial d_i}\Delta d_i + \frac{\partial\,{}^{i-1}\mathbf{A}_i}{\partial a_i}\Delta a_i + \frac{\partial\,{}^{i-1}\mathbf{A}_i}{\partial\alpha_i}\Delta\alpha_i \tag{10} $$

where $\Delta\theta_i$, Δd_i, Δa_i, and $\Delta\alpha_i$ are small errors in the kinematic parameters and the partial derivatives are evaluated with the nominal geometrical link parameters. From (1), taking the partial derivative with respect to θ_i, d_i, a_i, and α_i respectively, we can obtain

$$ \frac{\partial\,{}^{i-1}\mathbf{A}_i}{\partial\theta_i} = \begin{bmatrix} -s\theta_i & -c\theta_i c\alpha_i & c\theta_i s\alpha_i & -a_i s\theta_i \\ c\theta_i & -s\theta_i c\alpha_i & s\theta_i s\alpha_i & a_i c\theta_i \\ 0 & 0 & 0 & 0 \\ 0 & 0 & 0 & 0 \end{bmatrix}, \text{ and} $$

$\frac{\partial\,{}^{i-1}\mathbf{A}_i}{\partial d_i}, \frac{\partial\,{}^{i-1}\mathbf{A}_i}{\partial a_i}, \frac{\partial\,{}^{i-1}\mathbf{A}_i}{\partial\alpha_i}$ can be solved in the same way.

Let $d\,{}^{i-1}\mathbf{A}_i = {}^{i-1}\mathbf{A}_i * \delta\,{}^{i-1}\mathbf{A}_i$, and

$$ \delta\,{}^{i-1}\mathbf{A}_i = \mathbf{D}_{\theta_i}\Delta\theta_i + \mathbf{D}_{d_i}\Delta d_i + \mathbf{D}_{a_i}\Delta a_i + \mathbf{D}_{\alpha_i}\Delta\alpha_i \tag{11} $$

where $\mathbf{D}_{\theta_i}, \mathbf{D}_{d_i}, \mathbf{D}_{a_i}, \mathbf{D}_{\alpha_i}$ can be solved as follows:

$$\mathbf{D}_{\theta_i} = \left({}^{i-1}\mathbf{A}_i\right)^{-1} * \frac{\partial\, {}^{i-1}\mathbf{A}_i}{\partial \theta_i} = \begin{bmatrix} 0 & -c\alpha_i & s\alpha_i & 0 \\ c\alpha_i & 0 & 0 & a_i c\alpha_i \\ -s\alpha_i & 0 & 0 & -a_i s\alpha_i \\ 0 & 0 & 0 & 0 \end{bmatrix}, \text{ and}$$

$\mathbf{D}_{d_i}, \mathbf{D}_{a_i}, \mathbf{D}_{\alpha_i}$ can be got in the same way (12)

Expanding (11) into matrix form we can obtain

$$\delta\, {}^{i-1}\mathbf{A}_i = \begin{bmatrix} 0 & -c\alpha_i \Delta\theta_i & s\alpha_i \Delta\theta_i & \Delta a_i \\ c\alpha_i \Delta\theta_i & 0 & -\Delta\alpha_i & a_i c\alpha_i \Delta\theta_i + s\alpha_i \Delta d_i \\ -s\alpha_i \Delta\theta_i & \Delta\alpha_i & 0 & -a_i s\alpha_i \Delta\theta_i + c\alpha_i \Delta d_i \\ 0 & 0 & 0 & 0 \end{bmatrix} \quad (13)$$

The above expression gives the differential translation and rotation vectors for any type of joint as functions of the four D-H kinematic errors.

Similarly, for the proposed four degree-of-freedom carriage, the correct position and orientation of the task point p_4 with respect to the base frame due to the 4×4 kinematic errors can be expressed as

$${}^{0}\mathbf{A}_4^{c} = {}^{0}\mathbf{A}_4 + d\,{}^{0}\mathbf{A}_4 = \prod_{i=1}^{4} \left({}^{i-1}\mathbf{A}_i + d\,{}^{i-1}\mathbf{A}_i\right) \quad (14)$$

Expanding (14), and ignoring second and higher-order differential errors, then the relation between the differential change in carriage and the change in link parameters can be derived as

$$d\,{}^{0}\mathbf{A}_4 = \delta\mathbf{A}^1 * {}^{0}\mathbf{A}_4, \qquad \delta\mathbf{A}^1 = \sum_{i=1}^{4} \left([{}^{0}\mathbf{A}_i] * \delta\,{}^{i-1}\mathbf{A}_i * [{}^{0}\mathbf{A}_i]^{-1}\right) \quad (15)$$

where $\delta\mathbf{A}^1$ is the first order error matrix transformation in the fixed base frame. Following Paul [7], such a differential operator has the following form

$$\delta T = \begin{bmatrix} 0 & -\delta\theta_z & \delta\theta_y & \delta d_x \\ \delta\theta_z & 0 & -\delta\theta_x & \delta d_y \\ -\delta\theta_y & \delta\theta_x & 0 & \delta d_z \\ 0 & 0 & 0 & 0 \end{bmatrix} \quad (16)$$

If let $\delta\mathbf{X}_0 = \begin{bmatrix} \delta d_x & \delta d_y & \delta d_z & \delta\theta_x & \delta\theta_y & \delta\theta_z \end{bmatrix}^T \in \Re^{6\times 1}$ denote the positional and the orientation errors of the carriage, then from (15) and (16), it can also be rewritten as:

$$\delta X_0 = \sum_{i=1}^{4} \Delta\mathbf{x}_i = \sum_{i=1}^{4} \left(G_i \Delta\mathbf{y}_i\right) \quad (17)$$

where $\Delta\mathbf{x}_i = \begin{bmatrix} \delta dx_i & \delta dy_i & \delta dz_i & \delta\theta x_i & \delta\theta y_i & \delta\theta z_i \end{bmatrix}^T$ and $\Delta\mathbf{y}_i = \begin{bmatrix} \Delta\theta_i & \Delta d_i & \Delta a_i & \Delta\alpha_i \end{bmatrix}^T$, G_i is the identification Jacobian matrix.

B. Kinematic analysis and error modeling of Hexapod

Fig. 3 shows a schematic diagram of hexapod parallel mechanism, for the purpose of analysis, two Cartesian coordinate systems, frames $O_4(X_4, Y_4, Z_4)$ and $O_5(X_5, Y_5, Z_5)$ are attached to the base plate and the end-effector, respectively. Six variable limbs are connected with the base plate by Universal joints and the task platform by Spherical joints.

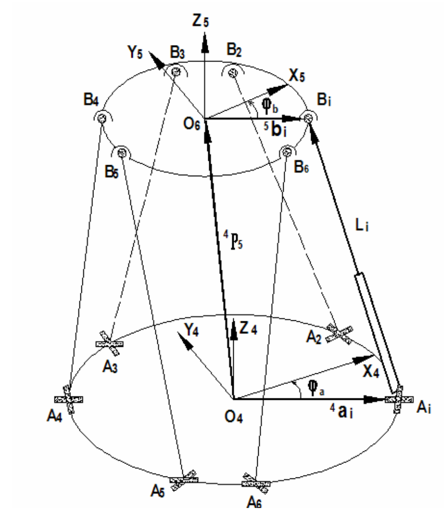

Figure 3. Norminal model of the Hexapod parallel mechanism

For the designed kinematics parameters, the following vector-loop equation represents the kinematics of the i^{th} limb of the manipulator

$$\overrightarrow{A_iB_i} = {}^{4}\mathbf{P}_5 + {}^{4}\mathbf{R}_5\, {}^{5}\mathbf{b}_i - {}^{4}\mathbf{a}_i \quad (\text{i}=1,2,3,4,5,6) \quad (18)$$

where ${}^{4}\mathbf{P}_5$ denotes the position vector of the task frame {5} with respect to the base frame {4}, and ${}^{4}\mathbf{R}_5$ is the Z-Y-X Euler transformation matrix expressing the orientation of the frame {5} relative to the frame {4},

$${}^{4}\mathbf{R}_5 = \begin{bmatrix} c\alpha c\beta & c\alpha s\beta s\gamma - s\alpha c\gamma & c\alpha s\beta c\gamma + s\alpha s\gamma \\ s\alpha c\beta & s\alpha s\beta s\gamma + c\alpha c\lambda & s\alpha s\beta c\gamma - c\alpha s\gamma \\ -s\beta & c\beta s\gamma & c\beta c\gamma \end{bmatrix} \quad (19)$$

and the ${}^{4}\mathbf{a}_i$, ${}^{5}\mathbf{b}_i$ represent the position vectors of U-joints A_i and S-joints B_i in the coordinate frames {4} and {5} respectively.

Let $\mathbf{l}_i$ be the unit vector in the direction of $\overrightarrow{A_iB_i}$, and l_i represents the magnitude of the leg vector $\overrightarrow{A_iB_i}$.

Differentiating both sides of (18) will yield

$$\delta l_i \mathbf{l}_i + l_i \delta\mathbf{l}_i = \delta\, {}^{4}\mathbf{P}_5 + \delta\, {}^{4}\mathbf{R}_5\, {}^{5}\mathbf{b}_i + {}^{4}\mathbf{R}_5 \delta\, {}^{5}\mathbf{b}_i - \delta\, {}^{4}\mathbf{a}_i. \quad (\text{i}=1,2,\ldots,6) \quad (20)$$

Let ${}^4\mathbf{R}_5\,{}^5\mathbf{b}_i = \mathbf{s}_i$, and multiply both sides of (20) with the unit direction vector $\mathbf{l}_i^T$, since $\mathbf{l}_i^T\mathbf{l}_i = 1$, $\mathbf{l}_i^T\delta\mathbf{l}_i = 0$ we can obtain:

$$\begin{aligned}\delta l_i &= \mathbf{l}_i^T\delta^4\mathbf{P}_5 + \mathbf{l}_i^T\delta^4\mathbf{\Omega}_5\times\mathbf{s}_i + \mathbf{l}_i^T\,{}^4\mathbf{R}_5\delta^5\mathbf{b}_i - \mathbf{l}_i^T\delta^4\mathbf{a}_i \\ &= \mathbf{l}_i^T\delta^4\mathbf{P}_5 + (\mathbf{s}_i\times\mathbf{l}_i)^T\,{}^4\mathbf{\Omega}_5 + \mathbf{l}_i^T\,{}^4\mathbf{R}_5\delta^5\mathbf{b}_i - \mathbf{l}_i^T\delta^4\mathbf{a}_i \\ &= \begin{bmatrix}\mathbf{l}_i^T & (\mathbf{s}_i\times\mathbf{l}_i)^T\end{bmatrix}\begin{bmatrix}\delta^4\mathbf{P}_5 \\ \delta^4\mathbf{\Omega}_5\end{bmatrix} + \begin{bmatrix}-\mathbf{l}_i^T & \mathbf{l}_i^T\,{}^4\mathbf{R}_5\end{bmatrix}\begin{bmatrix}\delta^4\mathbf{a}_i \\ \delta^5\mathbf{b}_i\end{bmatrix}\end{aligned} \quad (21)$$

Equation (21) can be rewritten as

$$\delta\mathbf{L} = \mathbf{J}_1\delta\mathbf{X}_1 + \mathbf{J}_2\delta\mathbf{P}_1 \quad (22)$$

where

$$\delta\mathbf{L} = [\delta l_1, \delta l_2, \delta l_3, \delta l_4, \delta l_5, \delta l_6]^T \in \Re^{6\times1} \quad (23)$$

$$\mathbf{J}_1 = \begin{bmatrix}\mathbf{l}_1^T & (\mathbf{s}_1\times\mathbf{l}_1)^T \\ \vdots & \vdots \\ \mathbf{l}_6^T & (\mathbf{s}_6\times\mathbf{l}_6)^T\end{bmatrix} \in \Re^{6\times6} \quad (24)$$

$$\mathbf{J}_2 = \begin{bmatrix}\left(-\mathbf{l}_1^T \quad \mathbf{l}_1^T\,{}^4\mathbf{R}_5\right) & \cdots & 0 \\ \vdots & \ddots & \vdots \\ 0 & \cdots & \left(-\mathbf{l}_6^T \quad \mathbf{l}_6^T\,{}^4\mathbf{R}_5\right)\end{bmatrix} \in \Re^{6\times36} \quad (25)$$

and

$$\delta\mathbf{P}_1 = \begin{bmatrix}\delta^4\mathbf{a}_i & \delta^5\mathbf{b}_i\end{bmatrix}^T \in \Re^{36\times1} \quad \imath=1,2,\ldots,6 \quad (26)$$

Since $\mathbf{J}_1 \in \Re^{6\times6}$ is a square matrix, and no singular points exist inside the workspace [3], $\mathbf{J}_1$ is invertible. Therefore, (22) can be written as:

$$\delta\mathbf{X}_1 = \mathbf{J}_1^{-1}\delta\mathbf{L} - \mathbf{J}_1^{-1}\mathbf{J}_2\delta\mathbf{P}_1 \quad (27)$$

The first term on the right side represents the errors induced by actuators and the second one is the position errors from the passive joints A_i and B_i .

C. Kinematic analysis and error modeling of the hybrid manipulator

The schematic diagram of the redundant hybrid manipulator is shown in Fig. 4, which is a combination of carriage and Hexapod manipulator mentioned above. The base plate frame {4} of Hexapod is coincided with the end task frame of the carriage. The global base frame {0} is located at the left rail.

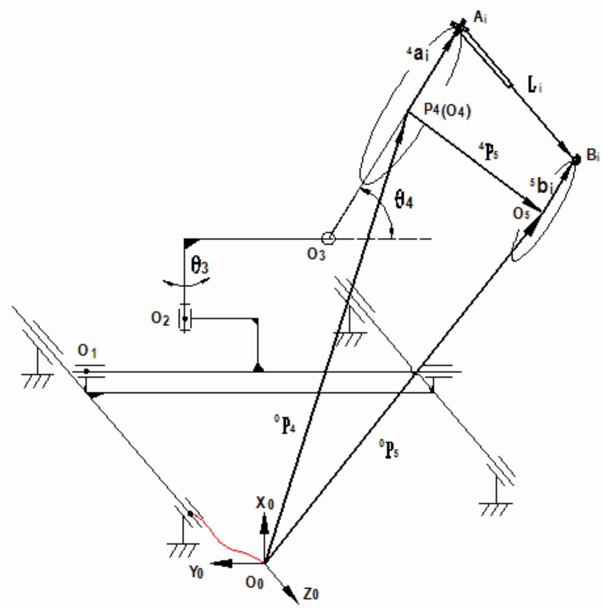

Figure 4. Schematic diagram of IWR

According to the geometry, a vector-loop equation can be derived as

$$\begin{aligned}{}^0\mathbf{P}_5 &= {}^0\mathbf{P}_4 + {}^0\mathbf{R}_4\,{}^4\mathbf{P}_5 = {}^0\mathbf{P}_4 + {}^0\mathbf{R}_4(l_i\mathbf{l}_i + {}^4\mathbf{a}_i - {}^4\mathbf{R}_5\,{}^5\mathbf{b}_i) \\ &= {}^0\mathbf{P}_4 + {}^0\mathbf{R}_4 l_i\mathbf{l}_i + {}^0\mathbf{R}_4\,{}^4\mathbf{a}_i - {}^0\mathbf{R}_5\,{}^5\mathbf{b}_i\end{aligned} \quad (28)$$

where ${}^0\mathbf{P}_5$ is the position vector of the task frame {5} (or end-effector) with respect to the fixed base frame {0}, and ${}^0\mathbf{R}_4$ is the rotation matrix of the frame {4} with respect to frame {0}.

Differentiating both sides of (28) and multiplying unit direction vector $\mathbf{l}_i^T$ yields

$$\begin{aligned}&\begin{bmatrix}\mathbf{l}_i^T & (\mathbf{r}_{bi}\times\mathbf{l}_i)^T\end{bmatrix}\begin{bmatrix}\delta^0\mathbf{P}_5 \\ \delta^0\mathbf{\Omega}_5\end{bmatrix} = \begin{bmatrix}\mathbf{l}_i^T & (\mathbf{r}_{ai}\times\mathbf{l}_i)^T + ({}^0\mathbf{R}_4 l_i\mathbf{l}_i\times\mathbf{l}_i)^T\end{bmatrix}\begin{bmatrix}\delta^0\mathbf{P}_4 \\ \delta^0\mathbf{\Omega}_4\end{bmatrix} \\ &+\mathbf{l}_i^T\,{}^0\mathbf{R}_4\mathbf{l}_i\delta l_i + \begin{bmatrix}\mathbf{l}_i^T\,{}^0\mathbf{R}_4 & -\mathbf{l}_i^T\,{}^0\mathbf{R}_5\end{bmatrix}\begin{bmatrix}\delta^4\mathbf{a}_i \\ \delta^5\mathbf{b}_i\end{bmatrix}\end{aligned} \quad (29)$$

where $\mathbf{r}_{bi} = {}^0\mathbf{R}_5\,{}^5\mathbf{b}_i$, $\mathbf{r}_{ai} = {}^0\mathbf{R}_4\,{}^4\mathbf{a}_i$

Equation (29) can be rewritten as

$$\mathbf{J}_3\delta\mathbf{X} = \mathbf{J}_4\delta\mathbf{X}_0 + \mathbf{J}_5\delta\mathbf{L} + \mathbf{J}_6\delta\mathbf{P}_1 \quad (30)$$

where

$$\mathbf{J}_3 = \begin{bmatrix}\mathbf{l}_1^T & (\mathbf{r}_{b1}\times\mathbf{l}_1)^T \\ \vdots & \vdots \\ \mathbf{l}_6^T & (\mathbf{r}_{b6}\times\mathbf{l}_6)^T\end{bmatrix} \in \Re^{6\times6} \quad (31)$$

$$\mathbf{J}_4 = \begin{bmatrix} \mathbf{l}_1^T & (\mathbf{r}_{a1} \times \mathbf{l}_1)^T + (l_i\, {}^0\mathbf{R}_4 \mathbf{l}_1 \times \mathbf{l}_1)^T \\ \vdots & \vdots \\ \mathbf{l}_6^T & (\mathbf{r}_{a6} \times \mathbf{l}_6)^T + (l_i\, {}^0\mathbf{R}_4 \mathbf{l}_6 \times \mathbf{l}_6)^T \end{bmatrix} \in \Re^{6\times 6} \quad (32)$$

$$\mathbf{J}_5 = \begin{bmatrix} \mathbf{l}_1^T\, {}^0\mathbf{R}_4 \mathbf{l}_1 & \cdots & 0 \\ \vdots & \ddots & \vdots \\ 0 & \cdots & \mathbf{l}_6^T\, {}^0\mathbf{R}_4 \mathbf{l}_6 \end{bmatrix} \in \Re^{6\times 6} \quad (33)$$

$$\mathbf{J}_6 = \begin{bmatrix} (\mathbf{l}_1^T\, {}^0\mathbf{R}_4 \quad -\mathbf{l}_1^T\, {}^0\mathbf{R}_5) & \cdots & 0 \\ \vdots & \ddots & \vdots \\ 0 & \cdots & (\mathbf{l}_6^T\, {}^0\mathbf{R}_4 \quad -\mathbf{l}_6^T\, {}^0\mathbf{R}_5) \end{bmatrix} \in \Re^{6\times 36} \quad (34)$$

Since $\mathbf{J}_3 \in \Re^{6\times 6}$ is a square matrix, and no singular points exist inside the workspace, $\mathbf{J}_3$ is invertible. Therefore, (30) can be rewritten as:

$$\delta\mathbf{X} = \mathbf{J}_3^{-1}\mathbf{J}_4\delta\mathbf{X}_0 + \mathbf{J}_3^{-1}\mathbf{J}_5\delta\mathbf{L} + \mathbf{J}_3^{-1}\mathbf{J}_6\delta\mathbf{P}_1 \quad (35)$$

where $\delta\mathbf{X} = \left[\delta\, {}^0\mathbf{P}_5 \quad \delta\, {}^0\mathbf{\Omega}_5\right]^T \in \Re^{6\times 1}$ denote the final output pose errors, and the first term on the right is the errors caused by the carriage, the second and third one represent the errors induced by the Hexapod machenism.

III. Simulations Results

In order to evaluate the final output errors caused by the error sources, a simulation example was performed using the following nominal parameters.

$$\left|{}^4\mathbf{a}_i\right| = 328mm, \left|{}^5\mathbf{b}_i\right| = 130mm, a_1 = 91mm, a_2 = 0,$$
$$a_3 = 252mm, a_4 = 354mm; d_3 = 331mm, d_4 = 0$$

Moreover, to estimate the accuracy of the derived error model, we assume a certain kinematics errors occurred in the carriage and Hexapod

$$|\delta\mathbf{L}| = 0.5mm, |\delta\mathbf{P}_1| = 0.1mm$$
$$|\Delta\alpha_i| = |\Delta\theta_i| = 0.1^\circ; |\Delta a_i| = |\Delta d_i| = 0.5mm$$

The range of the actuator input values are given in below, which will be generated by the random function in Matlab. The output position errors and orientation errors of the carriage, Hexapod and the whole robot in X, Y and Z direction for the 40 random generated poses are shown in Figure 5, 6, 7, 8,9,10 respectively. Figure 11 and Figure 12 illustrate the comparison of the absolute position and orientation error of carriage, Hexapod and the whole robot.

$$0 < d_1 < 800mm, 0 < d_2 < 300mm, 0^\circ < \theta_3 < 180^\circ,$$
$$0^\circ < \theta_4 < 90^\circ, 0^\circ < \alpha < 15^\circ, 0^\circ < \beta < 15^\circ, 0^\circ < \gamma < 10^\circ.$$

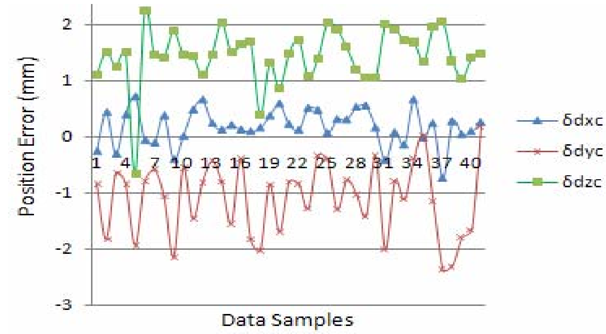

Figure 5. Position error of carriage in X, Y, and Z

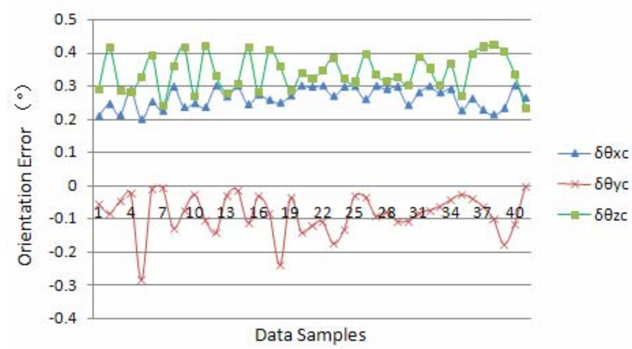

Figure 6. Orientation error of carriage in X, Y, and Z

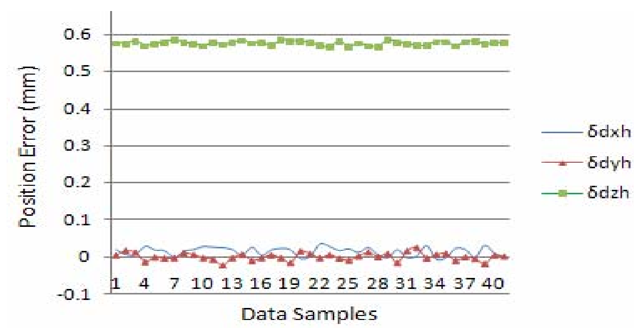

Figure 7. Position error of Hexapod in X, Y, and Z

Figure 8. Orientation error of Hexapod in X, Y, and Z

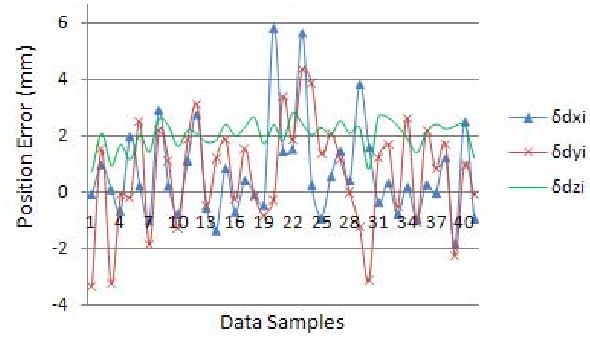

Figure 9. Position error of IWR in X, Y, and Z

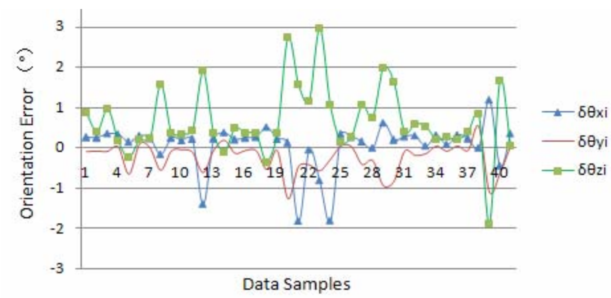

Figure 10. Orientation error of IWR in X, Y, and Z

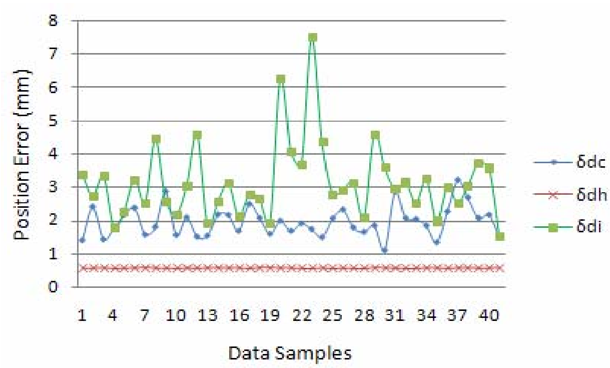

Figure 11. Comparison of the absolute position error of carriage, Hexapod and IWR

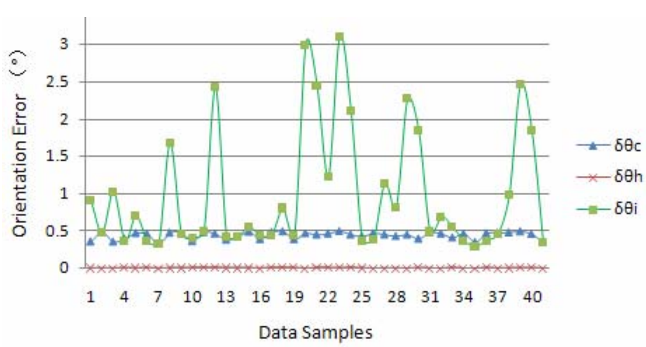

Figure 12. Comparison of the absolute orientation error of carriage, Hexapod and IWR

From these Figures it can be seen that the errors along Z axis are influenced significantly than that of X, Y axes, and the final output errors are not simply the superposition of the carriage and Hexapod. Comparing the absolute position and orientation errors of the carriage, Hexapod and IWR, we can see that the carriage error is the most important error sources to the final output errors, which causes about 80% of the whole errors. The final position errors are not greater than 10mm, which can be reduced to satisfy the accuracy requirement by means of some calibration methods in next step.

IV. CONCLUSIONS

In this paper, a hybrid redundant robot used for both machining and assembling of Vacuum Vessel of ITER is introduced. An error model derived for the proposed robot has the ability to account for the static sources of errors. Due to the redundant freedom of the robot, first we divide it into serial part and parallel part, and then formulate the error model respectively, finally combine them together to get the final error model. The error model has been simulated in Matlab and the results show that about 80% amount of errors in the end-effector is caused by serial link mechanism, i.e. carriage. In practice, to obtain desired accuracy of robot, these errors have to be reduced by further parameter identification methods. In the following work, efforts will be focused on the parameter identification using some optimization method to obtain desirable output errors.

ACKNOWLEDGEMENTS

This work, supported by the European communities under the contract of association between EURATOM and Finnish Tekes, was carried out within the framework of the European Fusion development Agreement. Authors from SLMT in China are grateful to the IMVE in Finland for the use of its research facilities and successful collaboration and China Scholarship Council for the partial financial support.

REFERENCES

[1] Huapeng Wu, Heikki Handroos, Pekka Pessi, Juha Kilkki, Lawrence Jones,"Development and control towards a parallel water hydraulic weld/cut for machining processes in ITER vacuum vessel". Int. J. fusion Engineering and Design, Vol. 75-79, pp. 625-631 , 2005.

[2] J. Wang and O. Masory,"On the accuracy of a Hexapod – part I The effect of manufacturing tolerances." IEEE Conf. on Robotics and Automation, pp. 114-120, 1993

[3] T.Ropponen. T.Arai,"Accuracy Analysis of a Modified Hexapod Manipulator". IEEE Conf. on Robotics and Automation, pp. 521-524, 1995

[4] W.K. Veitschegger, Chi-Haur Wu, " Robot analysis based on kinematics". IEEE J. Robotics and Automation, Vol. RA-2,NO.3, pp. 171-179, september, 1986

[5] Lung-Wen Tsai, Robot Analysis- the Mechanics of Serial and Parallel Manipulators. Wiley & Sons, New York, 2000.

[6] J.-W Zhao, K.-C Fan, T.-H Chang and Z. Li, "Error analysis of a serial-parallel type machine tool", Int J Adv Manuf Technol, Vol. 19, pp. 174-179, 2002

[7] R.P.Paul, Robot Manipulators:Mathematics, Programming, and Control, The MIT Press, Cambridge, MA, 1982.